

X-RAY STUDIES  
of  
BISMUTH  
SINGLE CRYSTALS

THESIS

by

Rudolf Clemens Hergenrother

In partial fulfillment of the requirements  
for the Degree of  
DOCTOR OF PHILOSOPHY

California Institute of Technology

Pasadena, California

1931

## TABLE OF CONTENTS

	Page
Abstract of Results	III
Introduction	
Previous Work	
Crystal Structure of Bismuth	1.
Allotropy of Bismuth	3.
Mosaic Structure of Bismuth	4.
Statement of Problem	4.
X-ray Studies of Bismuth Single Crystals	
Theoretical Consideration	
Interplanar Distances	5.
Energy Intensity of Bragg Reflection	
Structure Factor	7.
Ideal Crystals	9.
Mosaic Crystals	10.
Primary Extinction	11.
Secondary Extinction	12.
Debye Factor	13.
Effect of Parameter	13.
Experimental Procedure	
Preparation of Crystal Surfaces	16.
Measurement of Interplanar Spacing	19.
Determination of Parameter	
Photographic Measurements of X-ray Intensities	23.
Precision Photographic Method	24.
Measurements made with Precision Method	26.

	Page.
Ionization Method of Measuring X-ray Intensities	
Description of New Spectrometer	29.
Method of Measuring Integrated X-ray Intensities	39.
Discussion of Results	43.
Determination of Parameter	45.
Debye Factor	
Crystal Mounting	47.
Measurements	48.
Discussion of Results	49.
Numerical Value of $B$	50.
Discussion of Results	51.
Conclusion	52.
Bibliography	53.

## A B S T R A C T   O F   R E S U L T S

A new photographic method of measuring integrated intensities of x-rays reflected by crystals has been developed. The plate is calibrated with the same wavelength of rays as those measured. The exposures are adjusted so that each measurement produces about the same blackening of the plate. The resultant lines are measured by means of a microphotometer.

A new type of x-ray ionization spectrometer has been designed and was used for the present research problem. The ionization chamber is fixed and the ionization current is measured by means of a Hoffman electrometer, which makes it possible to measure x-ray intensities down to the lower limit imposed by cosmic rays and radio-active effects. By means of a precision adjustment the angle of the crystal can be adjusted to ten seconds of arc.

The lattice constant for the (111) plane of a bismuth crystal has been measured by the Siegbahn method and was found to be

$$D = 3.94531 \text{ \AA} \pm 0.00003 \text{ \AA} \quad \text{at} \quad (1)$$

23° Centigrade. The previous value given by James was

$$D = 3.95 \text{ \AA} \pm 0.08 \text{ \AA}$$

The lattice constant for the (11 $\bar{1}$ ) plane of a bismuth crystal was found to be

$$D = 3.73 \text{ \AA} \pm 0.01 \text{ \AA}$$

The parameter of the bismuth lattice was measured and was found to be

$$0.351 \text{ \AA} \pm 0.001 \text{ \AA} \quad \text{The} \quad (1)$$

previous value given by James was  $0.307 \text{ \AA} \pm 0.065 \text{ \AA}$

No difference was found between the lattices of bismuth crystals grown in a magnetic field and nonmagnetic bismuth crystals.

The lattice constants of the (111) planes are alike to within 0.0005%. The anomalous changes of density of bismuth single crystals grown in a magnetic field reported by Goetz and Focke<sup>(5)</sup> and the anomalous thermoelectric effects of these crystals reported by Goetz and Hassler<sup>(3)</sup> must be ascribed to changes in the secondary lattice structure.

The Debye temperature factor  $D$  for the reflection of x-rays of wavelength .708 Å from the bismuth (111) plane has been studied by making measurements of the integrated x-ray reflection for the third, fourth, and fifth orders in a temperature range from liquid air temperature to within 10 degrees Centigrade of the melting point of the crystal. A linear relation was found between the log of the integrated intensity and the square of the temperature which agrees with the theoretical expression

$$D = e^{-B \sin^2 \theta} \quad B = \alpha T^2$$

The dependence upon  $\theta$  was also checked.

It was found that at a temperature of ca. 70°C. this straight line shows a sudden change and continues in a linear relation of smaller slope. This was found for each order of reflection. No change was found in the primary lattice structure throughout this temperature range. This is interpreted as an indication of a pseudo-allotropic transformation occurring at this temperature. This checks the work of Cohen<sup>(6)</sup>, Moesveld and Cohen<sup>(7)</sup>, and Wurschmidt<sup>(8)</sup> who found anomalous density changes in bismuth in this temperature region which they incorrectly described as an allotropic transformation. The work of Goetz and Hassler<sup>(4)</sup> also shows an anomalous change in the thermoelectric power in this temperature region.

The lattice constant of the bismuth (111) plane was measured throughout this temperature range and it was found that the crystal has a constant expansion coefficient of  $14.0 \times 10^{-6}$  (25) from room temperature to  $255^{\circ}$  C. J. R. Roberts, using an intrefrometer method, found a value of  $16.2 \times 10^{-6}$  for this expansion coefficient. He found that this was constant up to  $230^{\circ}$  C. From this point on it gradually decreased to zero. A possible explanation of this discrepancy between the two results is that at  $230^{\circ}$  C. the secondary lattice structure becomes unstable and begins to degenerate. This would affect the measurements on the length of the crystal but would not affect the x-ray measurements of the primary structure. (26) P. W. Bridgman made a measurement of this expansion coefficient at room temperature and found the value  $13.96 \times 10^{-6}$  which is in agreement with my measurement.

## I N T R O D U C T I O N

The following paper is part of a research program concerning anomalies in the physical properties of metal single crystals, particularly bismuth, which are not explained by the present theories of solid bodies in general or by the present theories of the structure of crystals in particular.

In the present paper, x-ray crystal analysis measurements of bismuth single crystals are described. Two types of bismuth single crystals have been investigated. Ordinary bismuth has been known to exhibit certain anomalous physical properties, which have heretofore been ascribed to allotropic transformations. Bismuth single crystals grown in a magnetic field have been found to exhibit certain additional anomalous properties. The problem is investigated as to whether these effects are due to changes in the primary crystal lattice structure or whether they are indications of changes in the secondary lattice. The possible effect of secondary lattice structure upon the reflection of x-rays by a crystal is studied.

## PREVIOUS WORK

Crystal Structure of Bismuth

The crystal structure of ordinary bismuth has been studied by R. W. James <sup>(1)</sup> and by Hassel and Mark <sup>(2)</sup>. The crystal lattice was found to be rhombohedral (hexagonal system) and can be described as consisting of two similar intermeshed face centered rhombohedral lattices which are displaced relative to each other, along the trigonal axis. This displacement is referred to as the

lattice parameter.

(3)

A. Goetz has studied the effect of a magnetic field upon the crystallization of bismuth. This author found that if a bismuth single crystal is allowed to grow in a magnetic field the resultant crystallographic orientation is such that the direction of smallest magnetic susceptibility is parallel with the field. He also found that if the crystal is started growing with a different orientation before the field is applied, the subsequent application of the magnetic field produces no change in the original crystallographic orientation. The two parts of a bismuth single crystal grown under such conditions (half without a field and half with a field) were found to show different physical properties. The part of the bismuth crystal grown without a magnetic field is called the "normal" bismuth, and the part of the crystal grown in a magnetic field is called "magnetic" bismuth. The following anomalous properties of magnetic bismuth have been studied.

#### Thermoelectric Power

(4)

A. Goetz and M. Hassler have measured the difference in thermoelectric power for the normal and magnetic parts of bismuth single crystals. They found that this difference in thermoelectric power is greatest when the trigonal axis is parallel to the long axis of the crystal rod and perpendicular to the lines of force. They also found that the effect becomes a maximum in crystals which were grown in a field strength of 13,000 gauss. The effect appears to decrease with increasing purity of the bismuth. (The greatest amount of impurity, which consisted of lead, silver, and copper, was



probably less than 0.2% in their crystals).

#### Density

(5)

A. Goetz and A. B. Focke have found that the density of magnetic bismuth is greater than that of normal bismuth when the trigonal axis of the crystal is perpendicular to the lines of force and perpendicular to the long axis of the crystal rod. They have found that the density of the magnetic bismuth is smaller than that of the normal bismuth when the trigonal axis is perpendicular to the lines of force and parallel to the axis of the crystal rod. The changes in density are found to become smaller as the purity of the bismuth increases.

#### Allotropy of Bismuth

The existence of an allotropic form of bismuth with a transformation point in the neighborhood of 75 degrees Centigrade has been reported by Cohen<sup>(6)</sup>, Moesveld and Cohen<sup>(7)</sup>, and Wurschmidt<sup>(8)</sup>. These measurements were made with normal bismuth using dilatometric methods, a sudden decrease in volume being observed when the temperature changes from below 75 degrees to above 75 degrees Centigrade.

(4)

In the paper by Goetz and Hassler it is reported that the difference of thermoelectric power between normal and magnetic bismuth shows a linear relation to the mean temperature of the crystal except in the region of 72 to 82 degrees Centigrade, where the curve shows a sudden bend, giving a region of zero slope. This fact suggested to the above authors that the allotropic transformation mentioned above might enter into the thermoelectric power effects.

Mosaic Structure of Bismuth (9)

It has been found by A. Goetz that the (111) cleavage surface of a normal bismuth crystal shows a mosaic pattern of equilateral triangles the lengths of whose sides are found to be multiples of 1.4 microns. The above author interprets this as evidence of the regular mosaic structure which had been predicted from theoretical considerations by F. Zwicky (10,11).

STATEMENT OF PROBLEM

The papers dealing with the anomalous physical properties of bismuth single crystals grown in a magnetic field gave rise to a number of questions which are the subject of this paper.

The change in density of the magnetic bismuth reported by Goetz and Focke (5) suggested that the crystal structure of the magnetic bismuth might be different from that of normal bismuth in some way. This question was studied by making precise measurements of the Bragg angles of x-ray reflection from normal and magnetic bismuth crystals.

The lattice parameter of normal and magnetic bismuth were also compared by measurements of the intensity of x-ray reflection in various orders.

The problem of the determination of the mosaic crystal lattice and its effect upon the intensity of x-ray reflection through primary and secondary extinction was investigated.

A study was made of the crystal structure of bismuth at various temperatures from liquid air to within 10 degrees Centigrade of the melting point. In this way the Debye factor was determined,

which made it possible to compare the measured values of reflected intensities with the theoretical values. By this means also it was possible to decide whether the changes in the physical properties of bismuth in the neighborhood of 75 degrees Centigrade were due to changes in crystal structure or whether they were pseudo-allotropic effects. The existence of an ignition temperature for a pseudo-allotropic change was also investigated.

X - R A Y   S T U D I E S   O F  
B I S M U T H   S I N G L E   C R Y S T A L S

THEORETICAL CONSIDERATIONS

Interplanar Distances

The basis of all x-ray crystal structure work is the fact that the atoms of the crystal are arranged in a definite space lattice which is so perfect over an appreciable region that it acts as a three dimensional diffraction grating for x-rays which have a smaller wave length than the distance between the lattice planes. The space lattice of atoms can be described as sets of parallel equidistant planes of atoms. Constructive interference of the incident x-ray beam can only be produced when the angle of incidence  $\theta$  of the x-ray beam to one of these sets of atomic planes fulfills the Bragg Law

$$n\lambda = 2D \sin \theta$$

$n$  = order of reflection

$\lambda$  = wavelength of incident x-ray beam

$\theta$  = angle of incidence

$D$  = distance between successive atomic planes

When this condition is fulfilled for a particular set of atomic planes they act as a mirror to reflect a part of the x-ray energy. By using a known wavelength  $\lambda$  the spacing of a given set

of atomic planes in the crystal can be measured by determining the Bragg angle of reflection.

### Energy Intensity of the Bragg Reflection

The scattering of x-rays by the electrons in an atom can be dealt with successfully on the basis of classical electrodynamics as long as the electrons retain their positions in the atom during the process. In other words, such phenomena as Compton effect, photo-electric effect, etc., are ruled out. The phenomenon of the Bragg reflection of x-rays by a crystal lattice fulfills this condition approximately and can be handled accordingly. It should be emphasized that this method of treating the problem is only an approximation. Although the method has met with success in interpreting the measurements on the intensity of x-ray reflection from NaCl, its extension to atoms of very high atomic weights (with correspondingly high x-ray absorption) must be made with caution. It is, however, the only method of handling this problem at the present time.

#### X-ray Scattering by a Bound Electron

The intensity of the x-ray wave scattered by a single electron in the direction  $2\theta$  to a point at a distance  $r$  is given for an unpolarized incident beam of intensity  $I$  by the equation<sup>(12)</sup>

$$I_s = I \frac{e^4}{2r^2 m^2 c^4} (1 + \cos^2 2\theta) \quad [6.1]$$

$e$  = charge of electron

$m$  = mass of electron

$c$  = velocity of light

$2\theta$  = angle between incident and scattered ray.

## X-ray Scattering by an Atom

If we consider the diffraction of x-rays (which is a special case of scattering), by a layer of atoms in a crystal, the electrons in each atom will act as scatterers. If all the electrons of the atoms lay in the atomic planes, the energy intensity diffracted by one atom of atomic number  $Z$  would be  $ZI$ . Since the electrons in an atom are spread over a range of distances comparable with the spacing between the lattice planes, the waves sent out by electrons in different parts of an atom will be out of phase and produce interference which will diminish the resultant wave intensity.

The intensity of an unpolarized monochromatic x-ray beam diffracted at an angle  $2\theta$  by an actual atom is <sup>(13)</sup>

$$I_s' = F^2 I_s$$

$$I_s' = I F^2 \frac{e^4}{2r^2 m^2 c^4} (1 + \cos^2 2\theta) \quad [7.1]$$

$F$  = atomic structure factor.

A simple geometrical consideration will show that <sup>(14)</sup>

$$F = Z \int_{-a}^a p(z) \cos\left(\frac{4\pi z}{\lambda} \sin\theta\right) dz \quad [7.2]$$

$p(z)$  = probability of an electron being at a height between  $z$  and  $z + dz$  above the plane through the atom centers.

$\theta$  = angle of incidence of x-rays to the atomic plane.

$\lambda$  = wavelength of the radiation.

The value of  $F$  for the bismuth atom has been calculated <sup>(15)</sup> by L. Pauling on the basis of wave mechanics. He has been able to evaluate the probability  $p(z)$  in equation [7.2] by using hydrogen-

like eigenfunctions for each of the component electrons of the atom. Table #1 shows Pauling's values of  $F$  as a function of  $\sin \frac{\theta}{\lambda}$  for bismuth. Table #2 shows the values of  $F$  interpolated from this curve for the first seven orders of reflection from the bismuth (111) plane, of wavelength  $.708\text{\AA}$ , and the corresponding values for  $F^2 \left( \frac{1 + \cos^2 2\theta}{\sin 2\theta} \right)$

Table #1.

$\sin \frac{\theta}{\lambda}$	$F$
0.0	83.00
0.1	75.53
0.2	65.83
0.3	56.92
0.4	50.59
0.5	46.11
0.6	41.55
0.7	37.15
0.8	33.03
0.9	29.24
1.0	26.18

Table #2.

$n$	$\theta$	$\sin \frac{\theta}{\lambda}$	$F$	$F^2$	$\frac{1 + \cos^2 2\theta}{\sin 2\theta}$	$F^2 \left( \frac{1 + \cos^2 2\theta}{\sin 2\theta} \right)^{-3}$
1.	5.105°	0.1226	73.20	5,360	11.11	59.50
2	10.335°	0.2535	60.80	3,700	5.32	19.67
3	15.612°	0.3800	51.60	2,660	3.34	8.880
4	21.025°	0.5070	45.80	2,090	2.318	4.850
5	26.647°	0.6330	40.00	1,600	1.605	2.710
6	32.560°	0.7600	34.60	1,197	1.300	1.557
7	38.900°	0.8862	29.70	880	1.058	0.932

Fig. 2 is a graphical representation of Table #1 and shows the interpolation of  $F$  used in Table #2.

### X-ray Diffraction by a Small Ideal Crystal.

If we calculate the amount of energy diffracted by a small ideal crystal at absolute zero temperature, which is termed through the Bragg angle at a uniform rate  $\omega$ , and which is so small that the incident monochromatic unpolarized x-ray beam is not appreciably absorbed on passing through it, we arrive at the relation <sup>(16)</sup>

$$W = \frac{1}{2} \frac{I}{\omega} n^2 \lambda^3 F^2 \frac{e^4}{m^2 c^4} \left( \frac{1 + \cos^2 2\theta}{\sin 2\theta} \right) \delta V \quad [9.1]$$

$W$  = total energy diffracted or "integrated reflection"

$\omega$  = angular rate of turning of crystal.

$n$  = number of atoms per cubic centimeter.

$\lambda$  = wavelength of incident beam.

$F$  = atomic structure factor.

$I$  = incident x-ray intensity.

$\delta V$  = volume of small crystal.

$\theta$  = Bragg angle.

### X-ray Diffraction By A Thick Ideal Crystal.

If the same calculation is made for a thick ideal crystal, Darwin <sup>(17)</sup> and Ewald <sup>(18)</sup> have shown that the effect of the internal reflections is so great that the whole incident monochromatic x-ray beam is diffracted at the Bragg angle in a range of about five seconds of arc.

It is a significant fact that no crystal has ever been found to show such an effect. The crystals which approach this

condition closest are calcite and diamond. For the former, energy reflections of 40% of the incident monochromatic x-ray beam have been observed at the Bragg angle over a range of twelve seconds of arc.

Practically all crystals occurring in nature depart very widely from the ideal, having rocking angles (the angle through which the crystal shows any Bragg reflection) of from several minutes to several degrees.

#### Mosaic Crystals.

In order to obtain x-ray diffraction effects at all from a crystal it is necessary to have at least a small part of the crystal sensibly ideal. To fit this in with the theoretical considerations already discussed and the experimental fact of the existence of relatively large rocking angles in real crystals, Smekal, Ewald, and others have postulated the existence of the mosaic crystal. The structure of this mosaic crystal is thought by these authors to be the following. The crystal is built up of small blocks of arbitrary size. Each block is sensibly a small ideal crystal but adjacent blocks are slightly displaced relative to each other and this displacement destroys any phase relation between adjacent blocks and therefore causes each block to act independently of the others as far as diffraction is concerned. The angular displacement of the blocks is assumed to be statistical, and the deviation in angle from the mean therefore follows a Maxwell distribution curve. The rocking angle is a measure of the width (modulus) of this curve.

(11,12)

The Zwicky theory of secondary lattice structure postulates that the primary crystal lattice has superposed on it



a larger secondary lattice of  $\pi$  planes. In this way the primary lattice is divided into blocks which are in perfect alignment.

A mosaic crystal exhibits two new effects in x-ray diffraction.

#### Primary Extinction.

If the size of the mosaic blocks is small enough, each block will act like the small ideal crystal which has been discussed. If, on the other hand, the mosaic block is large enough so that an appreciable amount of internal reflection occurs, it has been shown by Darwin (19) that a phenomenon called "primary extinction" occurs, which introduces a multiplying factor  $\frac{\tanh m'q}{m'q}$  into the previous equation where

$$q = nFD\lambda \frac{e^2}{mc^2} \csc \theta \quad [11.1]$$

$D$  = lattice constant.

$n$  = number of atoms per cc.

$F$  = atomic structure factor.

$m'$  = number of atomic layers per block.

$\theta$  = Bragg angle.

The difficulty arises that no satisfactory method exists for the determination of  $M'$  the number of atomic layers per mosaic block, and no experiment has yet been devised for measuring the primary extinction directly.

There are three ways for determining whether a crystal exhibits primary extinction to an appreciable degree.

First: If two samples of the crystal differ widely in structure (degree of perfection of the crystal's surface) but still

give the same value of integrated intensity  $W$ , the primary extinction is small. This can be tested by measuring the integrated intensity for a good crystal surface and then disturbing the surface by grinding, and measuring again.

Second: The integrated intensity for a good crystal can be compared with the integrated intensity of the same crystal when it is finely powdered.

Third: If the primary extinction is an important factor,  $W$  should be proportional to  $F$  whereas if the primary extinction is negligible,  $W$  should be proportional to  $F^2$ .

#### Secondary Extinction.

The second type of phenomenon which the mosaic crystal exhibits is produced by the shielding effect upon the incident x-ray beam which the mosaic blocks in the upper layers produce upon the lower layers of the crystal. This is called "secondary extinction." This effect gives the crystal an increased absorption coefficient when it is turned to the region where the Bragg reflection occurs.

The theory of the secondary extinction has not been successfully treated, but it can be easily determined experimentally by measuring the integrated intensity for a series of different thicknesses of the same kind of crystal. Bragg, James, and Bosen-  
(20)  
quet have measured the secondary extinction coefficient for rock salt and have found that the coefficient decreases very rapidly with increasing order of reflection as is shown in Table #3.

Table #3.

Normal absorption coefficient of NaCl for  $.612\text{\AA}$  is 10.70

Order	Secondary ext. coeff.	Per cent of normal coeff.
1	5.6	52
2	1.96	18
3	0.02	0.18

#### Debye Factor

That the heat motion of the atoms in a crystal would impair the x-ray interference effects and decrease the intensity of x-ray reflection has been pointed out by Debye (21) and others.

The "Debye factor"  $D$  is the correction factor by which the reflection formula must be multiplied to represent the effect of temperature.

$$D = e^{-B \sin^2 \theta} \quad [13.1]$$

$\theta$  = Bragg angle.

(22)

The experimental measurements of  $B$  made by James and others do not agree quantitatively with the theoretical value but do agree qualitatively. Experimentally  $B$  is found to be independent of  $\theta$  and proportional to  $\frac{1}{\lambda}$  in agreement with theory. Also, at low temperatures  $B$  is found to be proportional to  $T^2$  in agreement with theory. However, at high temperatures the theoretical and measured dependence of  $B$  upon  $T$  is in general found to disagree. (c.f. James (22)).

#### Effect of Parameter.

If the crystal has a parameter (as is the case in bismuth) an additional effect will become apparent.

The x-ray interference effects produced by an interpenetration of two identical lattices will be the same, as far as

the Bragg angles is concerned, as that from either of the lattices alone. Since the lattices have a definite geometrical space relationship, the phase of the diffracted rays from the two lattices will have a definite phase relation, and their amplitudes will add vectorially. This phase relation will vary with the order of diffraction in the following way.

In the diagram, Fig. 1, let the solid lines 1 and 1' represent the plane perpendicular to the trigonal axis (Miller index (111), in the rhombohedral system) of one of the lattices of bismuth and the broken lines 2 and 2' represent the corresponding plane for the other lattice. Then  $\frac{b}{d}$  will be the lattice parameter. Let the x-ray beam be incident to these planes at the Bragg angle  $\theta_n$ . Since the phase difference of the waves from 1 and 1' is  $2\pi n$ , the phase difference between phase 1 and 2 will be  $\varphi = 2\pi n \frac{b}{d}$ . The interference between 1 and 2 will give

$$A^2 = 2 A_0^2 \left( 1 + \cos 2\pi n \frac{b}{d} \right) \quad [14.1]$$

$A_0$  = amplitude of wave reflected by either 1 or 2 if there were no interference between them.

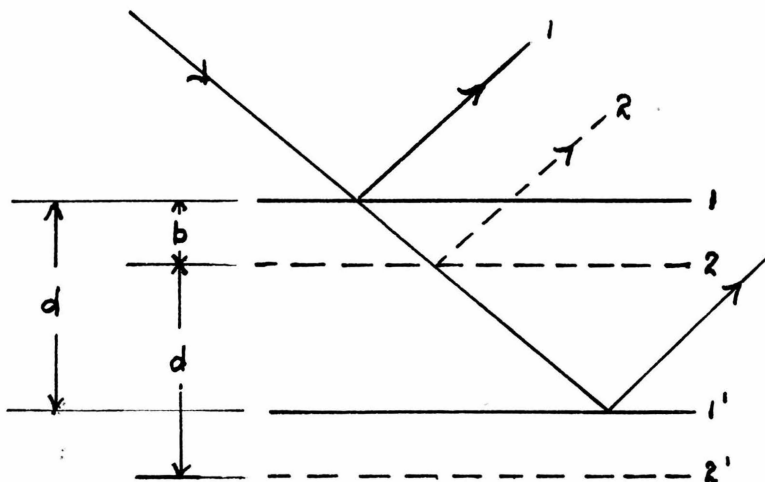


Fig 1

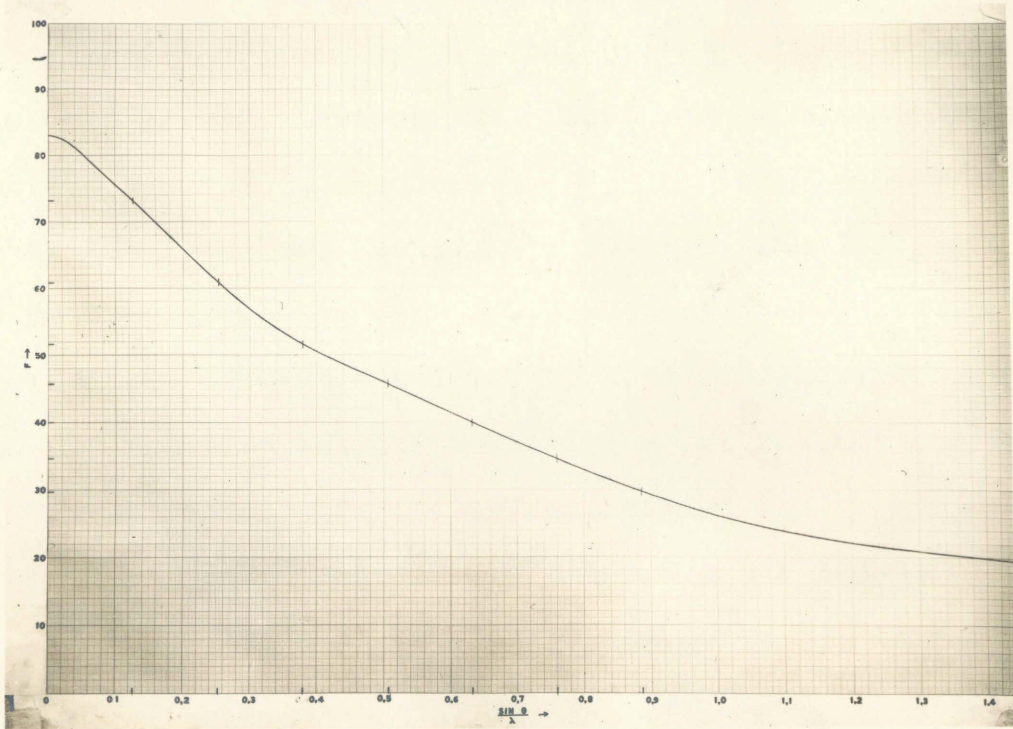


Fig. 2.

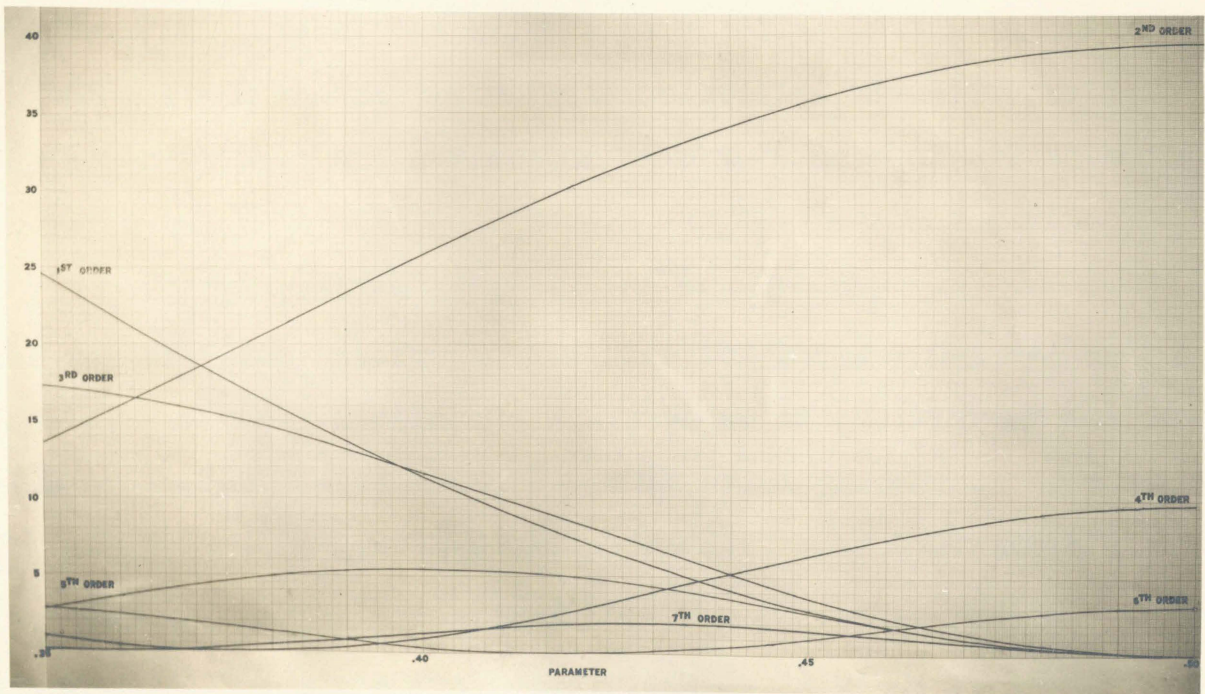


Fig. 3.

Fig. 3 shows the relative intensity for the first seven orders of Bragg reflection of wavelength  $.708\text{\AA}$  (Mo  $K\alpha$  line), from the (111) plane of the bismuth lattice, as a function of the parameters calculated by using equations [9.1] and [14.1], and the corresponding values of the structure factor interpolated from Pauling's data (Table #2 or Fig. 2). These values are calculated for the crystal at zero degrees absolute, and can be used for the interpretation of the measured integrated intensities by correcting these for temperature effect (Debye factor) and extinction.

## EXPERIMENTAL PROCEDURE

### Preparation of Crystal Surfaces.

The normal-magnetic bismuth single crystals which were studied were prepared after the method described by Goetz<sup>(3)</sup>. The type P<sub>3</sub> which shows the maximum difference in thermoelectric power between the two halves was used. In the P<sub>3</sub> orientation, the trigonal axis of the crystal is parallel to the long direction of the rod and the magnetic field is applied normal to this axis. The crystals used had a diameter of 3 to 4 mm. and a length of 10 to 12 cm.

The problem of preparing bismuth crystal surfaces which are suitable for use in the study of the Bragg x-ray reflection presented several difficulties. Because of the extreme softness and ease of distortion of these crystals, such procedures as cutting and grinding were not found to be feasible. The cleavage along the (111) plane, however, was found to be comparatively good, and that along the (11 $\bar{1}$ ) plane was found possible although it produced a rough-appearing step-like surface. The measurements of x-ray

reflection intensities were made primarily on the (111) plane prepared by cleaving the bismuth crystal. Tests were made of the cleavages at liquid air temperatures but this was not found to produce a better cleavage surface than when the cleaving was done at room temperature.

The method of cleaving was the following: The crystal was laid on a flat hardwood surface with a thin layer of soft wax under the region where the cleavage was to be made. A very thin, sharp razor blade was held parallel to the (111) plane (perpendicular to the long direction of the crystal for the P type) and the blade was given a sharp blow with a light hammer. The character of the cleavage surface was then examined under a low power microscope to determine its degree of perfection. It was found that in general the surface showed a curved portion for a distance of one-fourth or one-fifth of its diameter and that the rest of the surface was reasonably flat. A similar condition was found for large (5 mm. in diameter) and small (1.5 mm. diameter) crystals. It appeared as though the blade entered the crystal for about a fifth of its diameter and then the crystal suddenly broke over the rest of the surface and the two parts separated, moving a small distance apart and allowing the blade to go the rest of the way without touching either surface. The curved portion sometimes showed scratches from the blade, while the rest of the surface was generally free from scratches. Fig. 4 is a photograph of one of these cleaved surfaces. The purpose of the soft wax under the crystal was to prevent the two parts flying apart during cleaving.



Fig. 4. (x20)

The crystal was cleaved in this manner into pieces 2 to 3 mm. long, giving a total of about forty cleavages for a crystal. These cleavage surfaces were carefully examined under the microscope and the best surfaces selected from the normal and the magnetic half of the crystals. These selected surfaces were further compared by examining the image of a light source produced by a lens and reflected by the crystal surface upon a screen. The curved portion produced a broadened diffused spot on the screen whereas the rest of the surface produced a series of sharply defined spots. This indicated that the surfaces were generally composed of small reasonably flat facets which had slightly different orientations. The same test applied to naturally grown bismuth crystal faces showed an almost perfect image, showing that the natural crystal face is almost mirror-like. It was assumed that these distortions were produced by the shock the crystal



received during cleaving, and the existence of the facets would produce a wider rocking angle but would not affect the integrated intensity measurements, because of the large size of these facets (that is, their effect upon extinction would be nil). The best cleavage surface selected in this way from the magnetic and the best cleavage surface selected from the normal part of the crystal were subsequently studied by means of the Bragg x-ray reflection method.

#### Measurement of Interplanar Spacing.

For the first measurements, a Bragg type of x-ray spectrometer was used. The magnetic and normal bismuth crystals were mounted, one above the other, with the center line of their faces in the axis of rotation of the crystal holder. A lead Seemann type slit was adjusted to a distance of 0.3 mm. from the crystal surfaces. A molybdenum target x-ray tube, run at a voltage of 50 kv. in a current of 5 ma., was used as a source of radiation. The crystal holder was rocked back and forth at a uniform angle velocity through a large enough range to record the first five orders of Bragg reflection of the Mo  $K_{\alpha}$  lines on a photographic plate which was placed at a distance of 8 cm. from the axis of rotation and perpendicular to the primary x-ray beam. Exposures were made over periods of from 5 to 30 hours. After the exposure was completed, the plate was calibrated by exposing it to the direct primary rays for various periods of time. Fig. 5 shows a typical exposure taken with this apparatus.

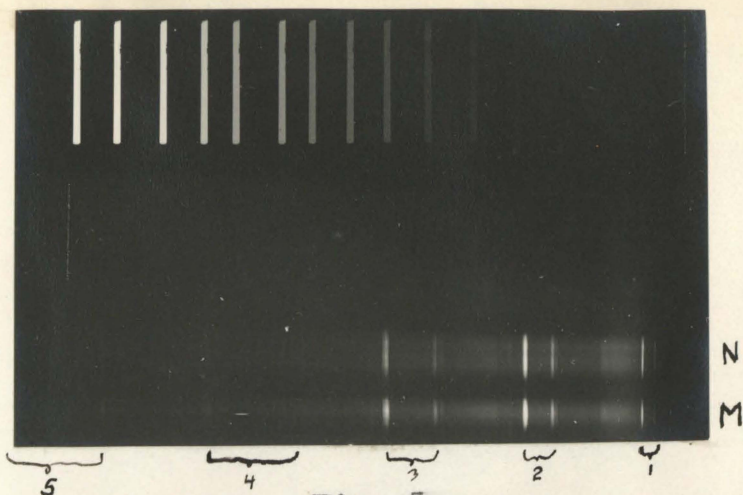


Fig. 5.

The lattice constant for the bismuth (111) plane and also of the  $(1\bar{1}\bar{1})$  plane deduced from the measurements of the Bragg angles from these plates agrees within experimental error (.5%) with the value given by James <sup>(1)</sup> (3.95Å), for both the magnetic and the normal bismuth.

In order to get a greater accuracy, some further measurements were made with a Siegbahn type of vacuum x-ray spectrometer <sup>(23)</sup>. The desirable feature of this type of spectrometer was the precision method of lining up the crystal, and the precision angle scale for measuring the position of the plate. This scale was calibrated in intervals of five minutes of arc, which were readable to a tenth part by means of two microscopes with vernier scales which were placed at diametrically opposite positions on the scale to eliminate the eccentricity error. A water cooled molybdenum target x-ray tube (Miller) was used as source of x-rays. This was run at 10 m.a. 57 k.v. with half-wave rectified a.c. voltage.

The lattice constant of magnetic and normal bismuth were measured, using the precision method developed by Siegbahn which is illustrated in Fig. 6.

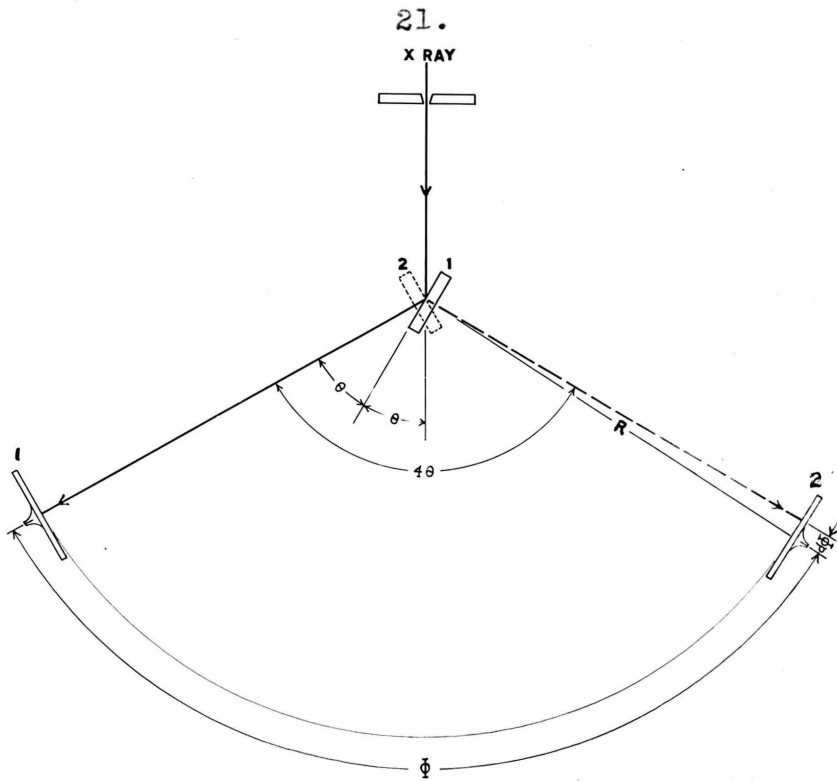


Fig. 6.

The crystal is turned to a position (1) to reflect a high order of the incident wavelength, and the plate holder is moved to such a position that the reflected ray will strike near the center of the plate. The angular position of the holder is carefully measured by reading the position of the precision scale with the two microscopes. The crystal is slowly turned through a small range of angle while the x-ray tube is operating to make certain of getting the reflection. The crystal is then moved to the position (2) and the plate is turned through an angle  $\Phi$  which is so chosen that the reflected ray will strike near the center of the plate close to the first image. The angle  $\Phi$  is determined precisely by another measurement of the position of the scale with the two microscopes (A and B). The distance  $R$  of the plate from the axis of rotation is carefully measured with a scale. The separation of the lines obtained on the plate is then measured on a comparator. This distance gives the quantity  $\delta = R d\Phi'$  from which  $d\Phi'$

(in radians) is determined. The equation

$$4\theta = \Phi + d\Phi$$

$$4\theta = \Phi + \frac{\delta}{R} \frac{360}{2\pi}$$

gives the value of  $\theta$  in degrees for  $d\Phi$  in degrees. Fig. 7 shows a print of the fifth order Mo  $K\alpha$  doublet reflected from a magnetic and a normal bismuth (111) plane.

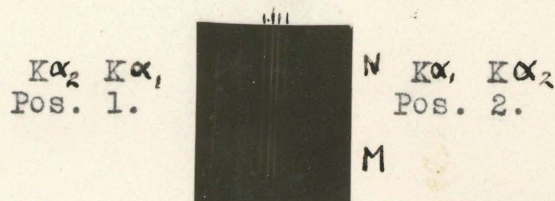


Fig. 7.

Comparator measurements of the plates give, as an average value of several measurements, the separation of Mo  $K\alpha$  lines, of 0.779 mm. for the normal bismuth and 0.777 mm. for the magnetic bismuth. These agree within the uncertainty of measuring the center of the line. If we take as an average value  $\delta = 0.778$  mm. we get

$$\delta = 0.778 \mp .001 \text{ mm.}$$

$$R = 172.6 \mp 0.2 \text{ mm.}$$

$$\Phi = 106.3292^\circ \mp .0035^\circ$$

$$4\theta = \Phi + \frac{\delta}{R} \frac{360}{2\pi} = 106.5877^\circ \mp .0035^\circ$$

$$\theta = 26.6469^\circ \mp .0009^\circ$$

Substituting this value for  $\theta$  in the Bragg Equation

$$n\lambda = 2D \sin\theta$$

$$n = 5$$

$$\lambda = .707768 \text{ \AA}$$

$$\sin\theta = .448487$$

we get

$$D = 3.94531 \text{ \AA} \mp .00003 \text{ \AA} \quad \text{at } 23^\circ \text{ Centigrade.}$$

The values given by James are for Bi (111) with Rh  $K\alpha$  ( $\lambda = .612\text{\AA}$ ) are

Table #4.

Order	$\theta_n$	$\sin \theta_n$	$\frac{\sin \theta_n}{n}$	Average $\frac{\sin \theta_n}{n}$
1	4° 29'	.07811	.07811	
2	8° 54'	.15471	.07735	
3	13° 26'	.23230	.07743	.07763 $\pm$ .00080

$D = 3.95\text{\AA} \pm 0.08\text{\AA}$

which agrees with our value.

It is thus proven that the magnetic and normal bismuth have identical lattice constants within .0005%. (It was not found feasible to prepare a good enough (111) bismuth facet for making a similar precision measurement. Since a previous measurement had shown agreement within 0.5% it was deemed highly improbable that a precision measurement would show any difference between magnetic and normal bismuth.)

#### DETERMINATION OF PARAMETER

##### Photographic Measurement of X-ray Intensities.

On the first set of measurements made with the photographic type of Bragg spectrometer it was observed that the relative intensities of the lines in different orders did not seem to agree for magnetic and normal bismuth. Accordingly, the intensity of the lines was measured by means of a recording microphotometer. By running the calibration region of the plate through the same photometer a calibration of the characteristic of the plate was obtained. From this calibration curve the intensity of the lines was interpolated. For x-rays in this wavelength range the blackening of the plate is proportional to the x-ray energy it receives. Table #5 gives the intensity values for the

various orders of reflection found by James<sup>(1)</sup> and the values determined from the measurements of three separate photographic plates.

Table #5.

Order	James's $\lambda = .612\text{\AA}$	Plate A		Plate B		Plate C		Average A,B,C	
		N	M	N	M	N	M	N	M
1	29	47	17.6	32.7	26.7			39.8	22.2
2	100	100	100	100	100	100	100	100	100
3	24	20.5	37.6	25.8	37.7	27.3	28.6	24.5	38.2
4	Not given	0.0	2.1	1.3	1.5	0.0	3.0	1.3	2.2
5	Not given	0.0	6.5	0.0	5.1	0.0	4.5	0.0	5.36

The first orders may be expected to show large variations because of the mechanical imperfection of the surfaces which introduces an error when the angle of incidence becomes small. The intensity for the second and third order for normal bismuth seems to agree with the values of James and the values for the magnetic bismuth seems to show a consistently different series of values. However, the variations between measurements are so great that these values are not to be trusted too much.

Precision Photographic Method of Measuring x-ray Intensities.

This apparent change in intensity of the integrated reflection seemed to indicate a possible change in parameter and for this reason it was decided to repeat the intensity measurements using a more accurate method.

A new method of making accurate x-ray intensity measurements with a photographic plate was devised. The Siegbahn

spectrometer was used for this purpose because the photographic plate could be moved to any predetermined position and the angular position of the crystal could be accurately adjusted. The new method makes use of the following principles.

1. To record a given order of Bragg reflection, the plate is fixed at a predetermined position and the crystal is turned at a definite angular speed past the Bragg angle from a position  $\theta - \psi$  to  $\theta + \psi$ , the range  $2\psi$  being chosen somewhat greater than the experimentally determined rocking angle.

2. To record successive orders of reflection, the plate is set at a series of successive positions which are chosen so that the respective reflected images are adjacent on the photographic plate.

3. For different orders, the x-ray tube voltage and current are maintained the same, but the angular speed of turning of the crystal is <sup>set</sup> for each case so that the blackness of the recorded lines of the different orders are nearly the same on the photographic plate. (It is assumed that the relative intensities are known roughly from a previous measurement.) These angular speeds are so adjusted that the blackness of the line corresponds to the linear part of the plate characteristic.

4. The plate is calibrated by turning the crystal to the order of reflection which is most intense and adjusting the crystal to a fixed position, where it gives a strong reflection. A number of exposures of this line are made for a series of different time intervals at successive positions of the plate.

The advantages of the method are the following:

1. The total angular turning distance of the crystal is very small compared with the total Bragg angle (usual method) thus giving a great economy of time of exposure.

2. The lines of successive orders are close together, which insures uniform characteristics of the plate and uniform treatment in development and fixing of the photographic plate. Having the lines close together also allows quicker and more accurate microphotometer measurements.

3. The adjustment of the angular speed of turning of the crystal can be done accurately by adjusting the speed of the driving motor. The relative opacities of the lines on the photographic plate can be determined with greater accuracy if the opacities are nearly alike and in the linear part of the plate characteristic than if they are widely different.

4. The calibration of the plate is made with the same wavelength as the lines to be measured. The width and intensity distribution of the calibration lines is the same as that of the lines to be measured, which makes the measurement independent of response characteristics of the microphotometer.

#### Measurements Made with Precision Method.

A number of normal magnetic bismuth crystals were studied by means of this method. Cleavage surfaces of the (111) plane were prepared and the normal and magnetic samples were mounted one above the other in the crystal holder so that both were measured simultaneously and the values of reflected x-ray intensity could be compared directly.



For a source of x-rays, a water cooled molybdenum target Müller x-ray tube was used. This was run at 10 m.a. and 57 k.v. The rotation of the crystal was accomplished by slow movement of an arm that was attached to the crystal holder. A d.c. shunt wound motor driving a 2,500 to 1 reduction gear whose end shaft unscrewed a nut which pushed a single ball bearing against a flat surface on the crystal arm holder was used. The speed of the motor could be varied by changing the armature voltage, which was constantly indicated by a voltmeter. The speed of the motor was accurately calibrated in terms of the armature voltage by means of a stroboscope which consisted of a white disk having a heavy radial black line, attached to the motor shaft, and a neon illuminator lamp operating on the 50 cycle a.c. lighting voltage.

Measurements of each of the first five orders of Bragg reflection were made. The ratios 1, 2, 4, 8, 16, 32, were used for the exposure times in these calibrations.

Four separate sets of normal magnetic samples were measured. For each plate, a calibration curve was plotted from the microphotometer readings taken on the calibration part of the plate. On this curve, the values of the measurements of the lines various orders of reflection was interpolated. The intensity of the background immediately adjacent to each line was also interpolated (this amounted to a quite small correction) and the true intensity was taken as the difference between line intensity and background intensity. Table #6 shows the measurements made on

4 plates. Fig. 8 shows a print from one of these plates.



Calibration 5 4 3 2 1

Fig. 8.  
Table #6.

Order	Plate D		Plate E		Plate F		Plate G	
	N	M	N	M	N	M	N	M
1	39.3	37.6	40.6	40.6	34.3	51.8	69.0	47.0
2	100	100	100	100	100	100	100	100
3	41.2	43.0	48.6	41.0	28.7	27.2	26.1	41.1
4	2.05	2.13			1.99	1.88	2.9	4.3
5	6.80	7.64	9.6	7.8	4.82	9.55	5.6	7.3

The data still shows considerable variation but does not indicate a systematic difference between magnetic and normal bismuth.

Plates D and E show the most consistent values. The large variation shown by different samples of crystal was rather puzzling since it did not appear possible that it could be explained by experimental error because of the great care with which the measurements were made and the apparent soundness of the method of measurement. The explanation for this variation was found later when a similar series of measurements were made using an ionization method of measuring the x-ray intensity. It was found that the integrated x-ray intensities were greatly dependent upon the character of the surface of the crystal.

Ionization Method of Measuring X-ray Intensities.

Description of a New Type of X-ray Ionization Spectrometer

Fig. 9 shows a drawing of the apparatus and Figs. 10a and 10b show photographic views from either side.

It will be noted from the drawing that the apparatus is a variation of the Bragg x-ray spectrometer, which differs from the usual type in that the x-ray tube is movable and the ionization chamber is fixed, instead of the reverse. Such a design was adopted because it was desired to measure small x-ray intensities by using a sensitive Hoffmann electrometer. This makes it desirable to use an evacuated connection between the ion chamber and the electrometer if the instrument is to be used at a high sensitivity. If the ion chamber is movable, a long movable connection is required but with a fixed ion chamber the connection can be made short and can be easily exhausted. For such a design it is, however, necessary to use an x-ray tube which can be operated with the center of the tube near ground potential. A Müller Metalix x-ray tube was used for this reason. This tube has its central part made of metal, which shields the x-rays from all directions except through a small window. The tube operates with the central metal part near ground potential (8,000 volts from central part to ground with 60,000 volts across tube).

The spectrometer (Fig. 9) has a fixed central post A, fastened to the base B. The upper part of the post is conical and carries a scale C which is clamped in an arbitrary fixed position; and the movable arm D. This arm carries at one end the x-ray tube holder E and a counterbalance W on the other end. An indicator fastened to this arm at the center measures its position

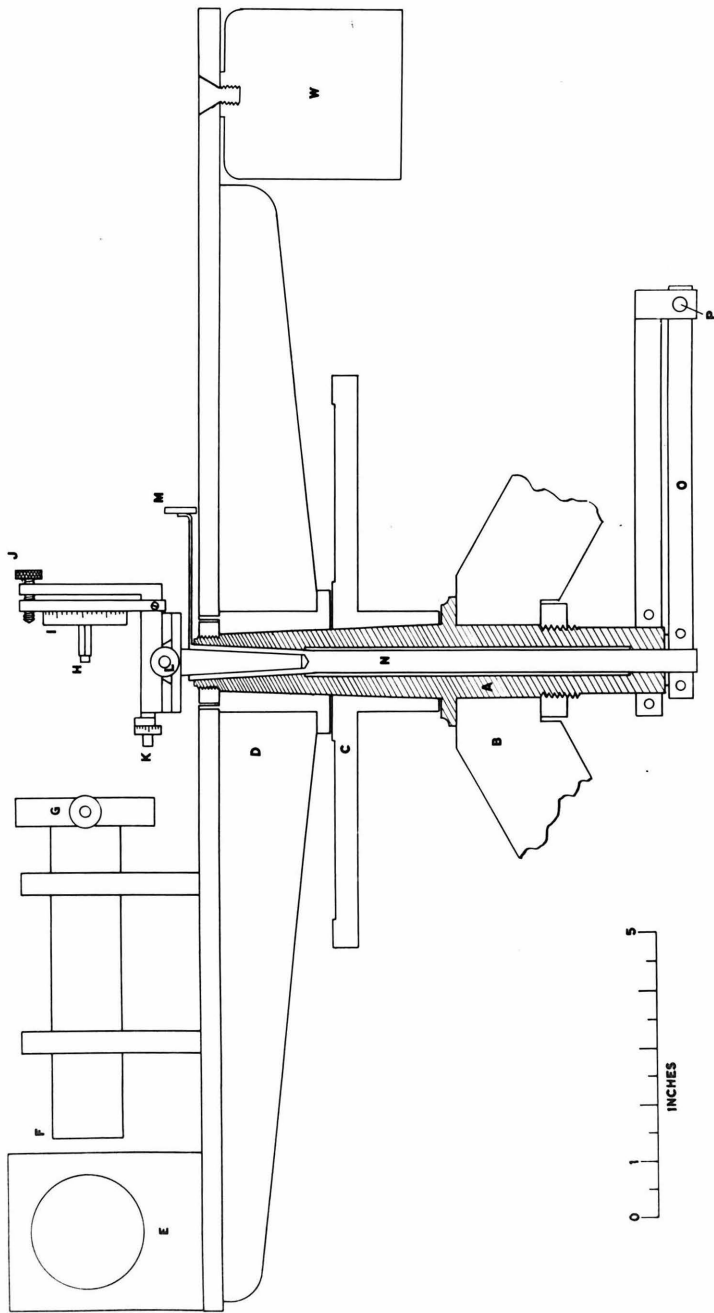
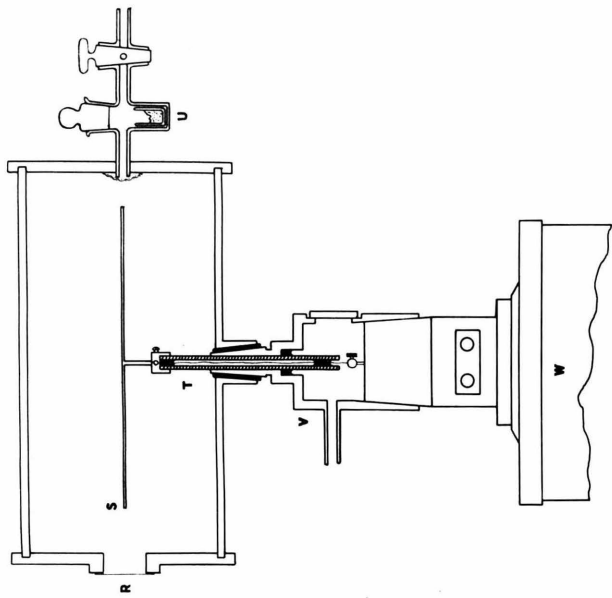


Fig 9

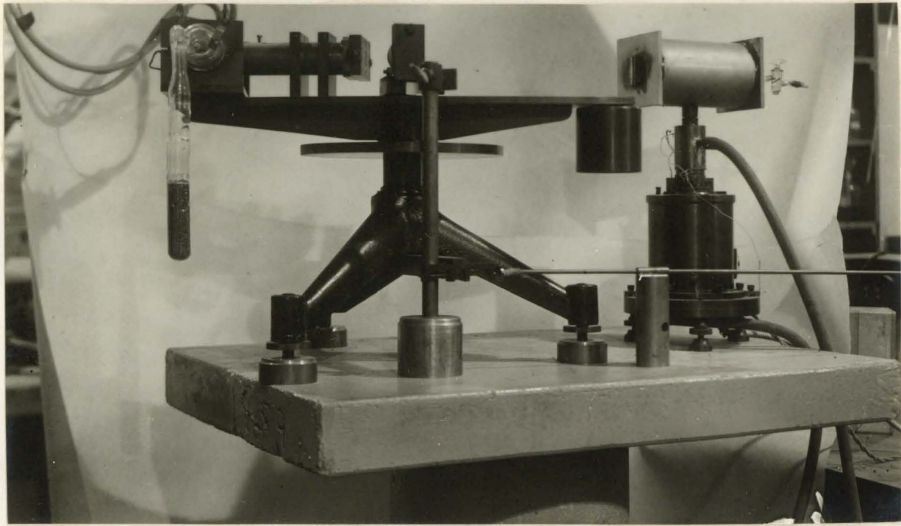


Fig. 10A.

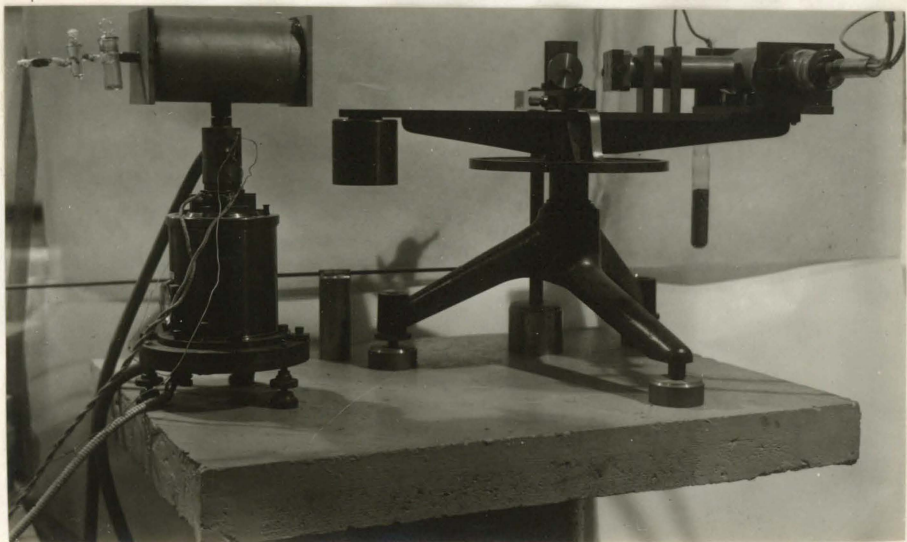


Fig. 10B.

relative to the scale C. A fixed slit F (.32 mm.) is on the x-ray tube end of the collimating tube and an adjustable slit G on the end next the crystal.

#### Crystal Holder Table.

The crystal H is mounted on a horizontal brass post  $\frac{3}{4}$ " long which holds the crystal far enough from the rest of the crystal holder table so that the incident x-ray beam does not strike it. The crystal holder has adjustments for five degrees of freedom. The rotation about an axis normal to the crystal face is read on scale I. A rotation about a horizontal axis parallel to the crystal face is accomplished by screw J, and the whole crystal table can be rotated about a vertical axis by turning the cone which supports it. Screws K and L allow transverse horizontal displacements of the crystal. Vertical displacement of the crystal is not required because the incident x-ray beam is much wider than the crystal face. An indicator fastened to the base of the crystal table measures its angular position relative to the scale C.

#### Rocking Angle Adjustment.

The crystal table can be turned as a whole through a range of two degrees by rotation of the shaft N which fits into a conical bearing in A. The lower end of N carries a lever arm O which is moved by the micrometer screw P. A long shaft with flexible coupling to P allows this adjustment to be made at a distance from the spectrometer. The upper end of N carries the mirror M whose angular position is accurately measured by a telescope and scale. In the original design, mirror M was

fastened to the lower part of shaft N but it was found that the twisting of the shaft caused an appreciable error in the reading of the position of the upper part of N. The present arrangement allows perfect duplication of angle readings to one-fifth second of arc.

#### Ionization Chamber.

The ionization chamber is filled with methyl bromide at atmospheric pressure. The chamber is made of brass which is nickel plated inside to prevent chemical action of the methyl bromide on the brass. The methyl bromide at this pressure absorbs 97% of the Mo  $K_{\alpha}$  radiation in traversing the length of the chamber. The window R consists of a piece of cellophane which is lightly coated with silver to make it conducting and thus electrically shield the opening. The size of the opening is  $3/16$ " x  $7/8$ ", which allows the two components of the Mo  $K_{\alpha}$  line to enter. The collector wire S is displaced to the side so the entering beam does not strike it. The wall of the ion chamber is at a potential of plus 45 volts above ground, which is above the saturation voltage (38 volts) of the ion chamber. Making its potential positive reduces the emission of photoelectrons by the remaining 3% of the entering x-ray beam which strikes the back of the chamber. The collector wire is supported on a quartz tube T which is cemented in the brass piece V, the latter being connected to the cover of the Hoffman electrometer W which is grounded. The piece T thus acts as a guard ring to prevent electrical leakage from the wall of the ion chamber to the collector wire. A fine wire (#40 to reduce electrical capacity of the system) runs down the center of the

quartz tube to connect the collector wire to the electrometer suspension. The tube U contains P O for drying the methyl bromide and the opening in the end of the ion chamber into which the glass tube is cemented is covered with a wire screen to complete the electrical shielding of the collector wire.

#### The Electrometer.

The Hoffmann electrometer was used to measure the ionization current. The suspension used had a half period of 12 sec. and was very nearly critically damped, the ratio of successive amplitudes of free vibration being 1 to 25. The electrometer was used with a binant voltage of  $10\frac{1}{2}$  volts, which gave a sensitivity of about 2,000 mm. per volt. The electrostatic capacity of the electrometer and ion chamber was not measured because this data was not needed, but it was known from measurements made on a similar apparatus that the capacity was roughly 15 cm.

#### Zero Background Drift.

The Hoffman electrometer was found to have a drift of 1 cm. on the scale in 16 seconds when the x-ray tube was not operating. This drift is referred to as the "zero Background" and represents the ionization produced by cosmic rays and by radioactive matter in the material of the ion chamber and its surroundings. That the effect is not spurious is proven by the fact that it disappears when the ion chamber is exhausted (prior to filling it with methyl bromide). The effect was found to agree in magnitude with the zero background observed by Archer Hoyt and Dr. J. Du Mond with a similar ion chamber and electrometer located in another part of the building.



The zero background was found to show a variation of 5% for successive readings of 10 cm. scale deflection. This is due to statistical variation of  $\alpha$  particles which produce many thousands of ions per cm. of path. The faintest x radiation accurately measured produced over four times this drift which reduced the variation to a little over 1% in this case. This variation is averaged out in the large number of readings taken for a single measurement of the integrated intensity.

#### Adjustment of Slits and Crystal.

The crystal to be studied was cemented to the small brass post (H, Fig. 9) which was screwed into I. For the purpose of accurately adjusting the slit G, a centerpost which fitted accurately into the conical hole in N was put in position in place of the crystal table. The upper end of this center post had been accurately ground to a tapering conical point, which was on the axis of the lower cone and consequently in the axis of rotation of the crystal. A small flashlight bulb was placed in front of F so that a beam of light would fall through slits F and G and cast a shadow of the conical point upon a white paper screen placed behind the point. The two sides of the slit G were then gradually closed to a separation of a few tenths of a millimeter until the shadow of the conical point fell in the center of the illuminated area. This assured that when the x-ray beam passed thru the slits F and G it would accurately pass through the axis of rotation of the crystal. A telescope with a vertical crosshair was placed at the same height as the center of the slit at a distance of about five feet. The telescope was then adjusted so that the image of the

cross hair co-incided with the image of the conical point, so that the image of the cross hair was in the axis of rotation of the crystal. The center post was then removed and replaced by the crystal table. The plane of the crystal face was adjusted parallel to the axis of rotation by turning the crystal table until the beam of light was reflected by the crystal face into the telescope. By turning screw J, the region of maximum intensity was brought into the center of the crosshair. The crystal table was then turned so that the crystal face was to the direction of the telescope and by transverse adjusting screw L the portion of the crystal that it was desired to study was brought into coincidence with the crosshair when viewed in the telescope. The crystal table was then turned through 90 degrees so that the crystal face was viewed on edge in the telescope and the transverse adjusting screw K was turned until the crosshair appeared just touching the crystal face. The adjustment was checked by turning the crystal table through 180 degrees and observing the tangency of the crosshair from the other side. The final check for accurate alignment of the crystal face with the axis of rotation was made by turning the crystal table slowly through the region where the light beam reflected by the crystal fell into the telescope field and observing that the telescope crosshair was accurately centered on the bright area which was reflected by the crystal face.

The angle scale C was adjusted so that when the arm D of the spectrometer and the ion chamber were in line, as is illustrated in Fig. 10, the indicator attached to arm D read zero on the scale. The position of the crystal table in Fig. 10 is arbitrarily turned

with respect to the arm D for simplicity of illustration. The scale C was subsequently clamped to post A and maintained in that position.

The measurement of intensity reflected by the crystal at the Bragg angle  $\theta$  was done in the following way: The arm D was turned through an angle  $2\theta$  (as shown by the indicator), so that the reflected x-ray beam would pass through the center of the ion chamber window. The micrometer adjusting screw P was set so that the arm O was midway between the stops and the crystal table was set into N in such a position that the indicator on the crystal table registered an angle  $\theta$  on the scale C. The x-rays were then turned on and the intensity of the reflected rays was observed by measuring the rate of drift of the electrometer. The position of maximum reflection was found by changing the angle of the crystal over a small range by means of the micrometer screw P (the position of arm O being read by means of the mirror M reflecting the image of a fixed scale into a telescope). This change in reading of the crystal table indicator on the scale C at this maximum showed the angle between the plane of the crystal face and the plane of I. The crystal table could now be re-adjusted so that the maximum reflection occurred when O was midway between the stops (indicated by the mirror M reflecting the center of the scale into coincidence with the telescope crosshair).

#### X-ray Shielding of Ion Chamber and Electrometer.

It was found necessary to shield the ion chamber with great care from stray x-rays. This was done by placing a  $3/32$ " thick sheet lead barrier (not shown in Fig. 9) between the spectrometer and the ion chamber. Between the window of the barrier and the

crystal, a 4" long brass tube having fixed lead slits was placed. These slits were open a distance of  $3/16$ " and served to decrease the solid angle subtended by the ion chamber window. In addition to these slits it was found necessary to put a lead baffle in line with the crystal and the ion chamber between the crystal and the x-ray tube. The size and position of the baffle was such that it was impossible to see the ion chamber window through the wide slits in front of it from any point around the x-ray tube. When this baffle was omitted it was found that the x-rays scattered from the air surrounding the x-ray tube reached the ion chamber in sufficient intensity to mask the fourth and higher orders of reflection from the crystal.

#### X-ray Tube Control and Measurement of Current and Voltage.

The x-ray tube was operated on half wave rectified a.c. (supplied by a Wappler Monex x-ray voltage supply). The x-ray filament current was supplied by a storage battery which was adjusted with a micrometer rheostat to give a constant emission current. The emission current was read by means of a multimeter before and after each electrometer measurement of ionization current to insure constancy. A series of measurements of x-rays reflected by a crystal were made with different x-ray tube currents and a linear relation (which was expected) was found. Because of the great range of x-ray intensities which were measured, two standard x-ray tube currents were used; 1 m.a. for strong reflections and 10 m.a. for weak x-ray reflections (fourth and higher orders). This made it possible to cover all ranges of intensity without changing the electrometer sensitivity. The primary supply voltage of the x-ray high voltage transformer was found to have a total

variation of 2% throughout a 24 hour period. It was found that this variation was at a minimum ( $\frac{1}{2}$ %) in the period from 10:00 p.m. to 3:00 a.m. Since the x-ray intensity depends upon the square of the voltage, a large variation in voltage can produce a serious error. For this reason, the measurements were made at the time when the line voltage was found to be steadiest, and, in addition, the transformer primary voltage was read before and after each electrometer deflection reading. A measurement was made of the x-ray intensity as a function of primary voltage and from this data each measurement of x-ray intensity of a given set of measurements was corrected to a standard primary voltage.

#### Method of Measuring Integrated X-ray Intensities.

The electrometer deflection was measured by the position of a light image reflected by the electrometer mirror on to a translucent celluloid scale. This scale was ruled in millimeter divisions and was curved so that the electrometer mirror lay at the center of curvature. The ionization current was determined by a stop-watch measurement of the time of transit of the electrometer scale image between two given points on the scale; that is, the time required to acquire the definite amount of charge. The ionization current was then proportional to the reciprocal of the period of time. The points chosen were 50 mm. from zero for the starting point and 150 mm. from zero for the end point. The error of this measurement was estimated to be not greater than  $\frac{1}{2}$  mm. or  $\frac{1}{2}$ %.

The crystal was first turned within a degree of the Bragg angle and a series of measurements of electrometer drifts was made. These measurements were found to be constant for various

positions of the crystal until the crystal was turned to a position within the rocking angle. For successive positions of the crystal the ionization current was found to increase up to a maximum value (Bragg angle) and was found to decrease again until the crystal was turned beyond the rocking angle where the ion current returned to its former constant value. This value is the x-ray background. The ionization current for each position of the crystal was computed by taking the reciprocal of the measured time of drift between two fixed points on the electrometer scale. From each of these values the ionization current of the x-ray background was subtracted. The resultant values were corrected to a standard primary voltage and plotted against the corresponding angular position of the crystal. The area of this curve was measured with an integrator and represents the total amount of x-ray energy given by Bragg reflection from the crystal for that particular order of reflection. This is referred to as "integrated x-ray intensity". The various orders of reflection for a given crystal were plotted for convenience on the same graph. The values of the abscissa (rocking angle) were taken arbitrarily as zero for the maximum point, although in reality the various orders of reflection occur at widely separated Bragg angles.

#### Measurements of Integrated Intensity.

Figs. 11A, 11B, 12A, and 12B show rocking angle intensity curves which were measured and plotted in the way described above. Planimeter Measurements of the areas under these curves are shown in Tables #6 and #7. The data in these tables is "normalized"; that is, multiplied by a factor so that the intensity of the second order is taken as 100.

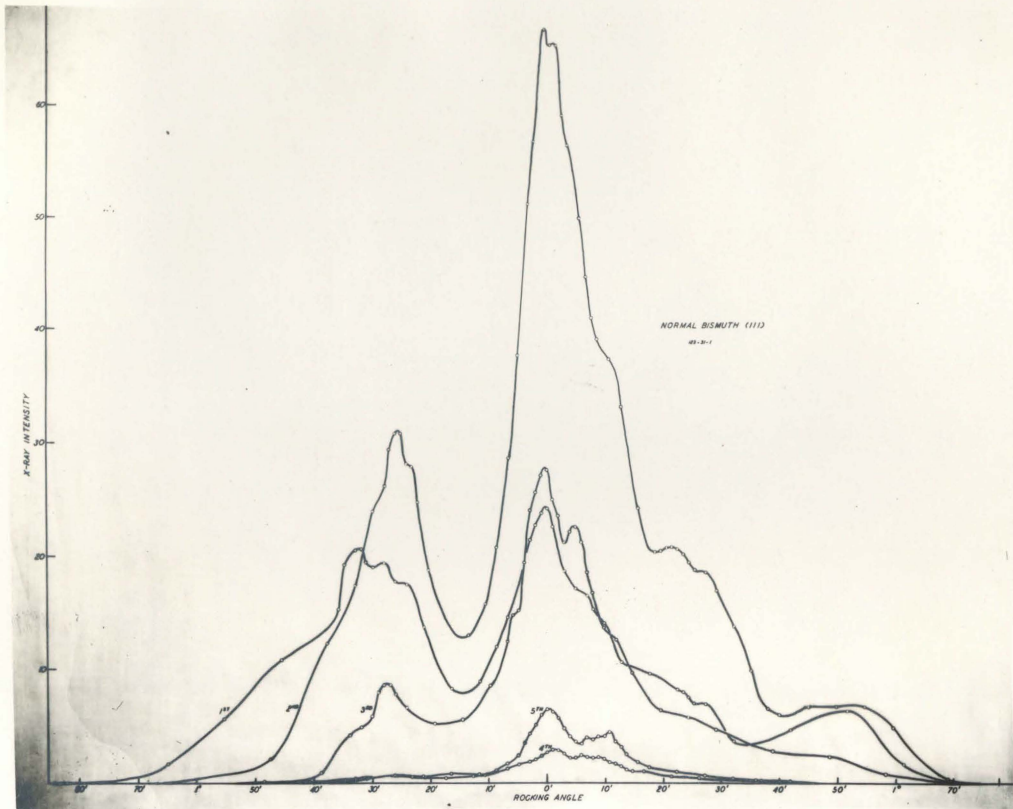


Fig. 12A.

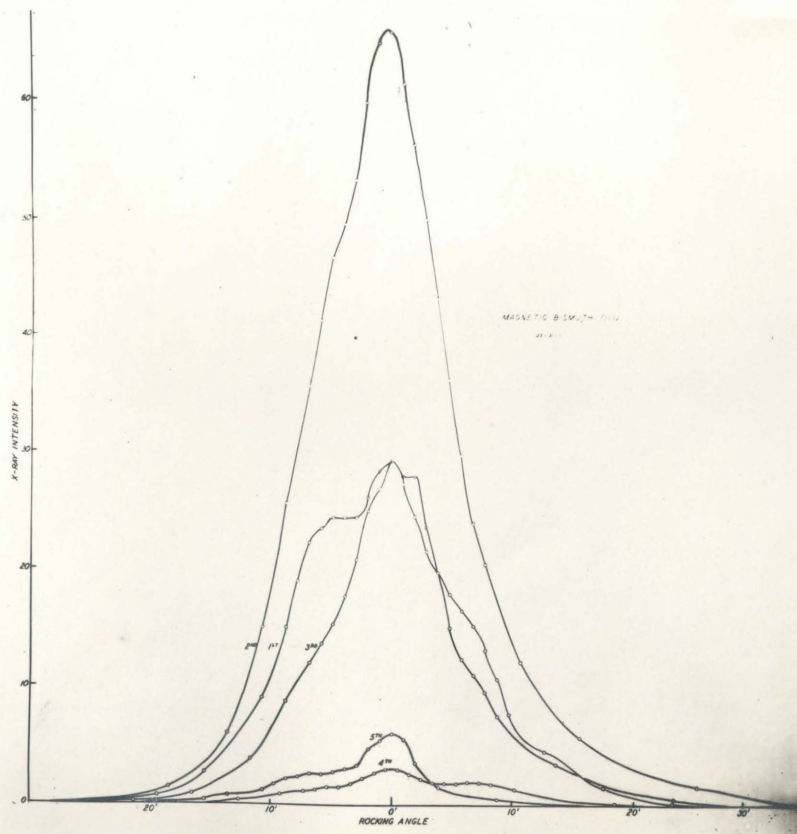


Fig. 12B

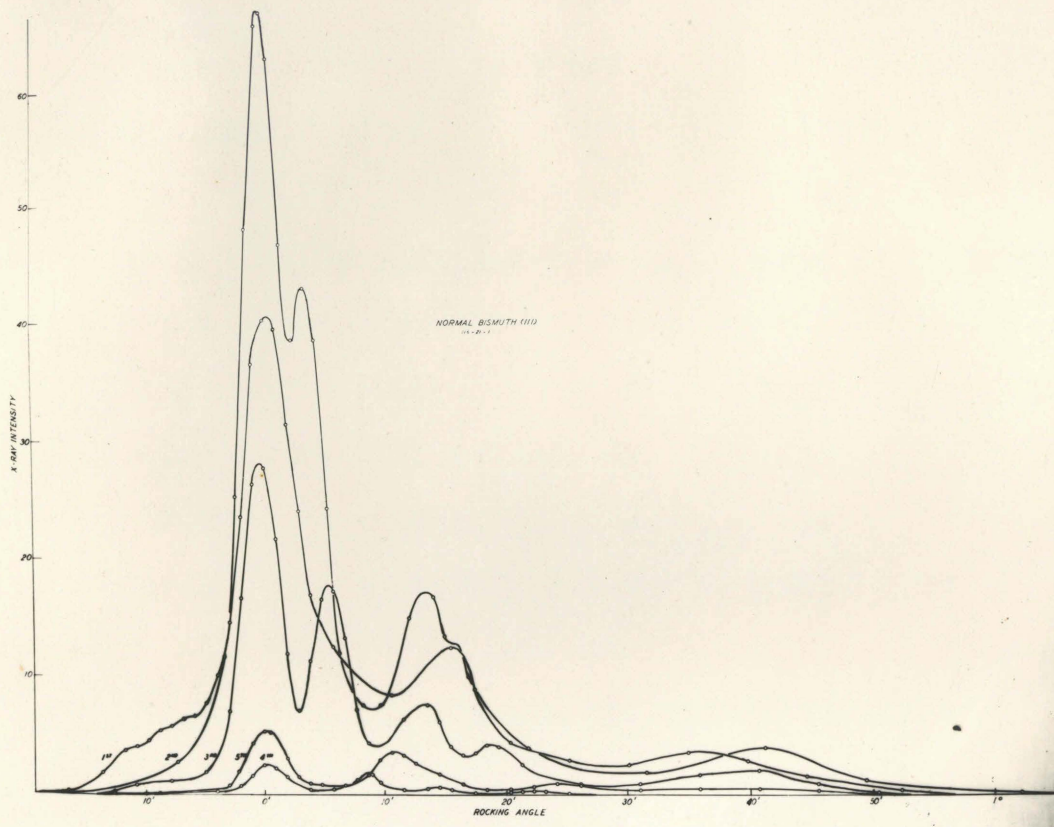


Fig. 11A.

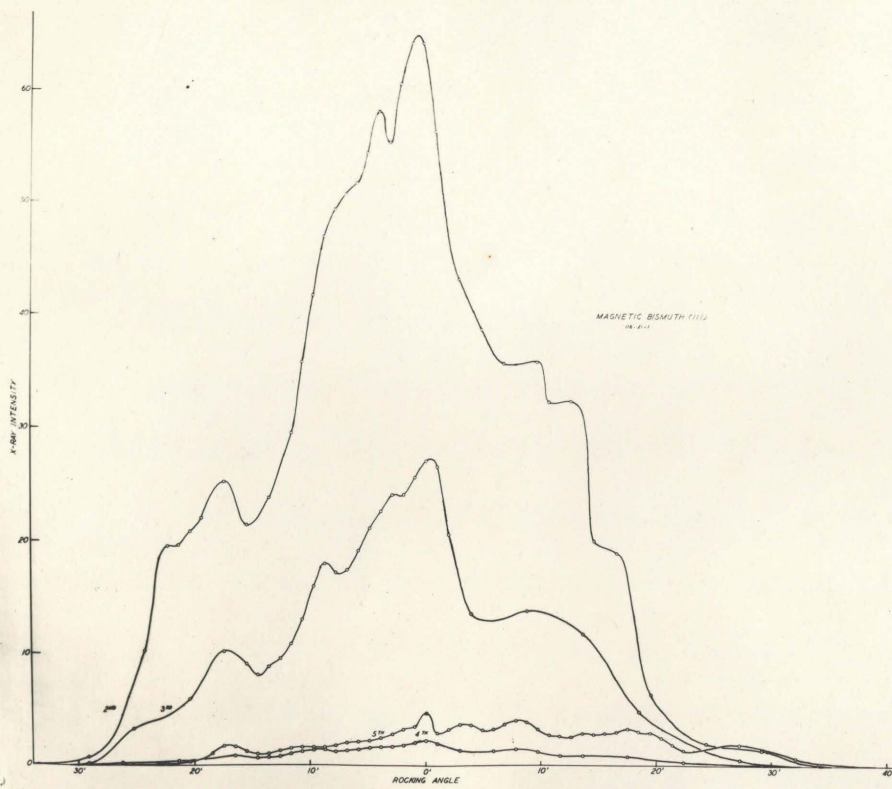


Fig. 11B.



Table #6.

(11A)			(11B)		
N			M		
Order	Area	Normalized	Order	Area	Normalized
1	534.4	77.5	1		
2	688	100	2	1625	100
3	300	43.5	3	621	38.2
4	22.8	3.31	4	54	3.32
5	66.8	9.70	5	117	7.17

Table #7.

(12A)			(12B)		
N			M		
Order	Area	Normalized	Order	Area	Normalized
1	780	66	1	487	40.5
2	1180	100	2	1201	100
3	400	33.9	3	417	34.7
4	36.8	3.11	4	45.1	3.75
5	65.0	5.50	5	90.1	7.50

#### Discussion of Results.

These measurements were taken with great care to reduce experimental error. The data plotted in 12A and 12B was checked by repeating the measurements on each set of data for each order. The respective measurements were found to agree within 1%. In addition to this, before each new set of observations was made, some of the previous measurements were checked to insure that nothing had changed in the meantime. The error of the integrated curve is estimated to be 1%.

The first order of Bragg reflection is not very reliable because of the small angle of incidence (5.1 degrees) of the incident beam. With a slit adjustment of 0.2 mm. the width of crystal surface reflecting x-rays in the first order is 2.2 mm. In this case any surface imperfections produce an appreciable effect on the x-ray reflection.

A study of curves 11A, 11B, 12A, and 12B and Tables #6 and #7 yields the following results:

1. The shape of the intensity-rocking angle curves shows that the crystal surfaces were composed of a number of comparatively large facets, each facet producing its own distribution curve and the resultant curve being the sum of all the separate curves. In the case of NaCl and similar crystals, these large facets are not found and their intensity-rocking angle curves are smooth and have only one maximum for each wavelength. When the resolving power is high enough, the Mo  $K\alpha$  lines become separated. An examination of the curves will show that this begins to happen in the second order and is already well pronounced in the third order. This is not to be confused with the additional maxima produced by other crystal facets. The effect of the resolution of the doublet and the reflection from other facets can be clearly distinguished by the fact that the former increases separation with increasing order, while the latter retains the same relative angular position in all orders.

2. If the integrated intensities (disregarding the first order) of normal and magnetic bismuth in Table #5 and also in

Table #7 are compared, it is not possible to account for the changes in intensities by changes in the parameter. This was determined by noting the direction in which the intensities would change for a change in parameter in the region of .41 of the plot of intensity against parameter (Fig. 3). No correspondence between the parameter curve and the intensity changes could be found.

3. A comparison of the maximum ordinates of different orders for the respective curves shows that these are in agreement within 2%. This agreement is significant considering the much greater range in values of the integrated intensities.

From these facts two conclusions are drawn:

First: The parameter of magnetic bismuth does not differ from that of normal bismuth.

Second: The integrated intensity depends upon the character of the surface. This is probably due to the very high x-ray absorption coefficient of bismuth for the wavelength used. The linear x-ray absorption coefficient is approximately 150. For the first order reflection the incident x-ray beam is reduced 9/10 in intensity by absorption alone in penetrating to a depth of about 2,000 atoms below the surface.

Determination of Parameter.

The shape of curve 12B shows that this had the best crystal surface of the group measured. For this reason the integrated intensities for this crystal will be used for determination of the parameter. The Debye factors that were obtained from an experiment to be described later give the following correction.

Table #8.

Order	Intensity	Debye Factor	Corrected Intensity
1	40.5	.978	41.4
2	100.0	.917	109.0
3	34.7	.760	45.6
4	3.75	.620	6.05
5	7.50	.445	16.85

Comparison of this set of corrected intensities with the parameter curve shows that the data fits best at a parameter of .411 if the position is chosen so that the agreement is best for the higher orders.

Table #9.

Parameter .410			Parameter .411		Parameter .412	
Exp. Value	Theor. Value	% Diff.	Theor. Value	% Diff.	Theor. Value	% Diff.
41.4	30.2	25	29.2	28	28.9	29
109.0	90.2	5.7	91.0	16	92.3	16
45.6	32.3	29	31.8	28	31.6	31
6.05	5.61	0.7	5.8	3.3	6.15	1.6
16.85	16.85	0.0	16.85	0.0	16.85	0.0

The parameter is defined by James <sup>(1)</sup> as the displacement in Å of one of the lattices from the center of the second lattice (parameter of 0.500 in notation used in this paper). In terms of the definition of James, the parameter is

$$(0.500 - 0.411) \times 3.945 \text{ \AA} = 0.351 \text{ \AA} \pm .001 \text{ \AA}$$

#### Effect of Extinction.

The measured intensities are greater than the theoretical values in the lower orders of Bragg reflection. This is contrary to

the way in which primary and secondary extinction would affect the reflection. This deviation seems to indicate the approximate character of the present status of the theory of x-ray crystal diffraction when it is applied to crystals having highly absorbing atoms.

#### DEBYE FACTOR.

#### Crystal Mounting.

A series of measurements of integrated x-ray intensities reflected by a bismuth (111) plane at various temperatures was made. For the purpose, the crystal was cemented with insolute into an electrically heated crystal holder, shown in Fig. 13.

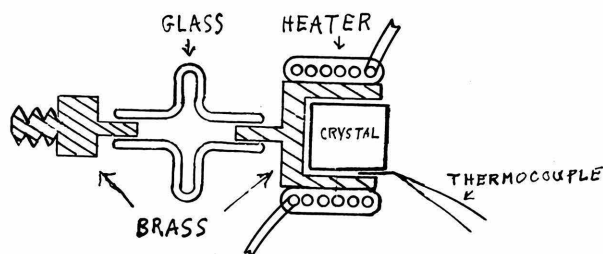


Fig. 13.

A storage battery with a control rheostat was used to adjust the temperature of the crystal. The temperature was read by means of a thermocouple which was cemented in position beside the crystal as shown. The thermocouple was calibrated for crystal surface temperature. The crystal could also be cooled to liquid air temperature. by means of a tiny jet of liquid air which was blown downward along the crystal face. By properly adjusting the rate of flow of liquid air, it was found possible to keep the crystal at liquid air temperature and to keep the reflecting face of the crystal "wet" with a thin film of liquid air and perfectly bright and free

from  $\text{CO}_2$  or water crystals. During these measurements, the surface of the crystal was continually observed by means of a telescope and mirrors to insure that the face of the crystal was kept free.

#### Relation of Maximum Intensity to Integrated Intensity.

A number of measurements of integrated intensity were made for a crystal at room temperature and at a temperature of  $255^\circ \text{C}$ . It was found that the curves were similar and the integrated area of the curves was proportional to the maximum height. The subsequent measurements were made by determining the maximum intensities of reflection for each particular temperature.

#### Measurements.

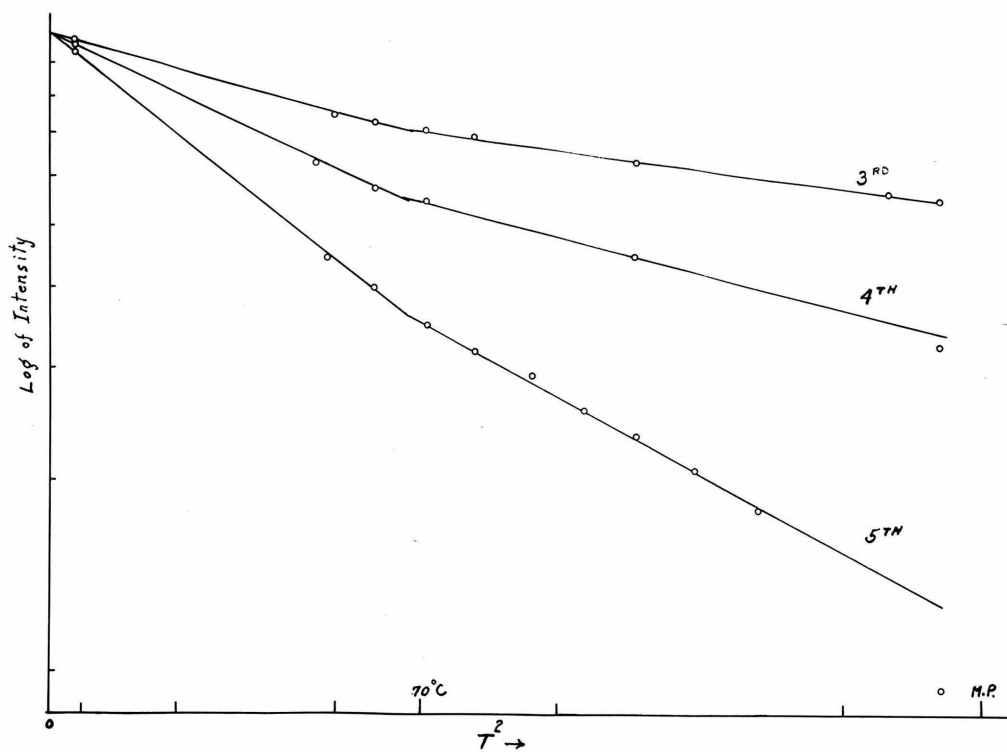


Fig. 14.

Fig. 14 shows the results of a series of measurements made in this way on a bismuth (111) cleavage plane. The log of the integrated intensity was plotted against  $T^2$  which should give a linear relation if  $B$  in the Debye factor is proportional to  $T^2$ .

It was found possible to measure the expansion of the lattice directly by measuring the change in the Bragg angle. This amounted to about 1 mm. change in the rocking angle scale reading at the maximum point for a change of  $60^\circ$  C. The scale could be read to about a fourth of a millimeter, but the position of the maximum could not be measured so precisely because of the width of the peak. The error of this measurement was estimated at 5%.

#### Discussion of Results.

The results shown in Fig. 14 indicate that the curves consist of two linear parts which intersect in the neighborhood of  $70^\circ$  C. This is an indication that something changes in the crystal at this temperature. The temperature at which the change seems to occur agrees with the temperature at which Cohen<sup>(6)</sup>, Moesveld and Cohen<sup>(7)</sup>, and Wurschmidt<sup>(8)</sup> observed an anomalous expansion for polycrystalline bismuth. It also agrees approximately with the temperature (72 to  $80^\circ$  C.) at which Goetz and Hassler<sup>(4)</sup> observed the anomalous thermoelectric power for normal-magnetic bismuth single crystals. On the basis of this evidence it appears that at this temperature ( $70^\circ$  C.) there may be a kind of ignition temperature for a pseudo-allotropic change occurring in the secondary lattice structure.

#### Expansion Coefficient.

The lattice structure does not change and the measurements of the change in Bragg angle indicate that the expansion

coefficient of the lattice is constant throughout the range of the temperature studied. The expansion coefficient was found to be

$$14.0 \pm 0.7 \times 10^{-6}$$

(25)

J. K. Roberts measured the expansion coefficient of bismuth perpendicular to the (111) plane by means of an intreferometer method and found the value  $16.2 \times 10^{-6}$ . A very significant fact is that he found the expansion coefficient began to decrease rapidly at about  $230^{\circ}$  C. and fell to 0 just before the melting point. He regarded this as an indication of the breaking down of the crystal lattice. My measurements were made on the lattice planes directly and show that the primary lattice does not break down up to a temperature of  $255^{\circ}$  C. An explanation of this difference which correlate the two is that at  $230^{\circ}$  C. the secondary lattice structure (Zwicky <sup>(10,11)</sup>) becomes unstable and possibly goes into what may be described as a molten condition. A point which supports this view is that in Fig. 14 the intensities at the highest temperature measured ( $255^{\circ}$  C.) fell below the straight line curve for the fourth and fifth orders. (The third order may have an experimental error at this point.) The falling off may be an indication of the melting of the secondary lattice.

#### Numerical Value of B

The values of the Debye factor at room temperature taken from the curve Fig. 14 are given in the following table.

Table #10.

n	D	log D	sin <sup>2</sup> θ	B = - $\frac{\log D}{\sin^2 \theta}$	
3	.760	-.2744	.0722	3.81	Average B 3.89 ± 0.16
4	.620	-.4780	.1285	3.73	
5	.445	-.8088	.201	4.02	



The agreement is good considering that measurements were made at only one low temperature point (liquid O<sub>2</sub>).

#### DISCUSSION

A complete discussion of results has already been given at the end of each topic, which is recorded in the Table of Contents. Instead of repeating this, the following discussion will be formulated in a very general way.

Bismuth single crystals grown in a magnetic field are known to exhibit anomalous changes in density, electrical conductivity, and thermoelectric power. X-ray crystal structure measurements of these crystals prove that the primary crystal lattice remains unchanged throughout the anomalous changes in physical properties. This proves that it is necessary to ascribe these changes to something other than the primary lattice and gives support to the theory of secondary crystal lattice structure.

Ordinary bismuth is known to exhibit anomalous density changes in the neighborhood of 70° C. which have been ascribed to an allotropic transformation. Studies of x-ray reflections from bismuth single crystals as a function of temperature reveal that the primary lattice is unchanged and that a pseudo-allotropic transformation occurs near 70° C. This pseudo-allotropic transformation may be interpreted as a change in the secondary lattice structure. Measurements of the linear expansion of bismuth crystals seems to indicate that the secondary lattice begins to degenerate when the temperature exceeds 230° C. X-ray measurements indicate that the primary lattice shows no degeneration in its structure up to 255° C.

In conclusion, I wish to express my appreciation to Dr. A. Goetz for his guidance and inspiration throughout the course of this research work and also to Dr. R. A. Millikan for the interest he has shown.

I am also indebted to Messrs. A. B. Focke and M. F. Hassler for their work in growing the crystals which were used. Dr. J. Dumond, Mr. Archer Hoyt, and Dr. L. Pauling have given valuable help and suggestions on questions bearing on this research problem.

## BIBLIOGRAPHY

- |     |   |                         |            |      |           |
|-----|---|-------------------------|------------|------|-----------|
| 1.  | R. W. James                                     | Phil. Mag.              | <u>18</u>  | 193  | (1921)    |
| 2.  | Hassel and Mark                                 | Zeit. f Phys.           | <u>23</u>  | 269  | (1924)    |
| 3.  | A. Goetz  | Phys. Rev.              | <u>35</u>  | 193  | (1930)    |
| 4.  | A. Goetz and M. F. Hassler                      | Phys. Rev.              | <u>36</u>  | 1752 | (1930)    |
| 5.  | A. Goetz and A. B. Focke                        | Phys. Rev.              | <u>37</u>  | 1044 | (1931)    |
| 6.  | E. Cohen  | Akad. Amst. Verls.      | <u>23</u>  | 1224 | (1914-15) |
| 7.  | A. Moesveld and E. Cohen                        | Zeit. f Phys. Chem.     | <u>85</u>  | 420  | (1913)    |
| 8.  | J. Wurschmidt                                   | Verk. d. Dt. Phys. Ges. | <u>16</u>  | 799  | (1914)    |
| 9.  | A. Goetz  | Proc. Nat. Acad. Sci.   | <u>16</u>  | 99   | (1930)    |
| 10. | F. Zwicky                                       | Proc. Nat. Acad. Sci.   | <u>15</u>  | 816  | (1929)    |
| 11. | F. Zwicky                                       | Proc. Nat. Acad. Sci.   | <u>15</u>  | 753  | (1929)    |
| 12. | X-rays and Electrons, Compton                   | Page 60, Equation       |            |      | (3.04)    |
| 13. | X-rays and Electrons, Compton                   | " 122, "                |            |      | (5.06)    |
| 14. | X-rays and Electrons, Compton                   | " 122, "                |            |      | (5.07)    |
| 15. | L. Pauling                                      | Zeit. f Krystall.       |            |      | (1931)    |
| 16. | X-rays and Electrons, Compton                   | Page 125, Equation      |            |      | (5.15)    |
| 17. | C. G. Darwin                                    | Phil. Mag.              | <u>26</u>  | 675  | (1914)    |
| 18. | P. P. Ewald                                     | Phys. Zeit.             | <u>26</u>  | 29   | (1925)    |
| 19. | C. G. Darwin                                    | Phil. Mag.              | <u>43</u>  | 800  | (1922)    |
| 20. | Bragg, James, & Bosanquet                       | Phil. Mag.              | <u>41</u>  | 309  | (1921)    |
|     |   |                         | <u>42</u>  | 1    | (1921)    |
| 21. | P. Debye  | Ann. d. Phys.           | <u>43</u>  | 49   | (1914)    |
| 22. | R. W. James                                     | Phil. Mag.              | <u>49</u>  | 505  | (1925)    |
| 23. | Spektroskopie der Roentgenstrahlen, M. Siegbahn |                         |            |      |           |
| 24. | S. K. Allison & A. H. Armstrong                 | Phys. Rev.              | <u>26</u>  | 701  | (1925)    |
| 25. | J. R. Roberts                                   | Proc. Roy. Acad. Sci.   | <u>106</u> | 385  | (1924)    |
| 26. | P. W. Bridgman                                  | Proc Nat. Acad Sci.     | <u>10</u>  | 411  | (1924)    |